Annals of Biomedical Engineering, Vol. 35, No. 3, March 2007 *(© 2006)* pp. 397–407
DOI: 10.1007/s10439-006-9221-6

The Adhesion Between a Microvillus-Bearing Cell and a Ligand-Coated Substrate: A Monte Carlo Study

JIN-YU SHAO and GANG XU

Department of Biomedical Engineering, Washington University, One Brookings Drive, St. Louis, MO 63130-4899, USA

(Received 4 May 2006; accepted 17 October 2006; published online 7 December 2006)

Abstract—In biology, specific cell adhesion is mediated by receptor–ligand interactions. Consequently, its strength correlates with the strength of single receptor–ligand bonds that can be measured with a variety of techniques. However, whether single receptor–ligand bonds are truly present in an experiment is often a concern. In this paper, we present a Monte Carlo simulation of the adhesion between a microvillus-bearing cell and a ligand-coated substrate. In the simulation, ligands were immobilized on the substrate either uniformly or in clusters of three and seven, while receptors were distributed uniformly on the microvillus tip and they moved randomly on the cellular surface. How ligand clustering affects the adhesion frequency and forward rate constant was studied. Other factors that were studied include receptor aggregation on the microvillus tip, ligand density, receptor density, contact time, and binding pocket size. In the case of uniformly distributed ligands, our simulation results agree well with those obtained from probabilistic analysis. We found that, even with clustered ligands on the substrate, most of the adhesion events were mediated by a single bond if the total adhesion frequency was less than 20%. Besides, ligand clustering decreased the total adhesion frequency and forward rate constant, but increased the single-bond adhesion frequency under comparable conditions. These findings should lend us some assistance in identifying single bonds in cell–substrate or cell–bead adhesion measurements and in illustrating some biological mechanisms that involve clustered ligands.

Keywords—Single-bond, Ligand clustering, Adhesion frequency, On rate, Off rate, Forward rate constant.

INTRODUCTION

Adhesion is ubiquitous in biological processes. In some cases such as cell–cell junction, cell locomotion, and cell growth, strong adhesion is necessary. In some other cases such as leukocyte rolling on the endothelium, weak or temporary adhesion is sufficient. Specific adhesion in biology and medicine is usually mediated by receptor–ligand interactions. Therefore, the strength of single receptor–ligand bonds is of great interest to biophysicists and bioengineers. Many seminal experimental studies have been conducted since atomic force microscopy, optical trap, and other techniques emerged in the nineties.[28,31] However, whether single receptor–ligand bonds are truly present in an experiment is often a concern. A single bond, i.e., two bound molecules only tens of nanometers in size, cannot be visualized under a microscope unless sophisticated optical technology is employed. Consequently, observable or measurable signatures of single bonds such as low adhesion frequency, quantal behavior, and single-bond kinetics have often been used for identifying them. Although these signatures do point in the direction of single bonds, they do not guarantee single bonds because many other factors such as multivalency, protein clustering, and surface heterogeneity may come into play.[31]

A receptor–ligand bond is often studied between a cell and a ligand-coated substrate or bead. In this type of experiment, the cell is allowed to contact the substrate for a known amount of time and then pulled away with a force imposed by flow-induced shear stress, mechanical cantilever, optical trap or other means. During the contact, although ligands are immobile, receptors undergo a perpetual Brownian motion. Close contact between the cell and substrate still allows receptors to diffuse on the cell.[7] If adhesion occurs between the cell and substrate, it can be detected by the development of an adhesive force evidenced, e.g., by a cantilever deflection as in atomic force microscopy or by a decrease in the velocity of the cell over the substrate as in the slow rolling of a leukocyte in a parallel flow chamber. The number of receptor–ligand bonds formed during the contact depends mainly on receptor mobility and density, ligand mobility and density, contact time, contact area, and reaction rate constant.[1,6]

Address correspondence to Jin-Yu Shao, Department of Biomedical Engineering, Washington University, One Brookings Drive, St. Louis, MO 63130-4899, USA. Electronic mail: shao@biomed.wustl.edu

One approach to interpreting this type of experiment is to analyze the kinetics of small systems with probabilistic analysis.[5,18,21,31] With this approach, Chesla et al.[4] and Piper et al.[21] found that the likelihood of having a single bond in the contact area was very high if the overall or total adhesion frequency, which was defined as the number of adhesion events divided by the number of trials, was less than 20%. A Monte Carlo (MC) simulation, in which receptors and ligands were both monovalent and uniformly distributed on the cell and substrate, also showed that this criterion was very dependable.[25,26] For more complex situations such as clustering or multivalency, the criterion of low adhesion frequency may not be applicable.[31] In this paper, to examine the effect of clustered ligands on this criterion, we present a Monte Carlo simulation for the adhesion between a ligand-coated substrate and a microvillus-bearing cell like a human neutrophil.

The advantage of MC simulation over theoretical kinetic analysis lies with its relatively easy implementation and its capacity to readily model and track molecular-scale events such as individual protein movement and interaction even in theoretically challenging situations like clustering and multivalency. MC simulation has been successfully applied to the study of reaction, diffusion, protein activation, and other processes in biological systems.[11,14–17,22–24] It has also been successfully applied to the study of the role of ligand clustering in controlling the overall receptor occupancy on a cell.[13] In an earlier simulation of cell–substrate adhesion,[25,26] receptor–ligand bonds were assumed to have very long lifetimes and cell surface roughness was ignored. In this paper, with all these factors included in our simulation, we first validate our MC simulation by comparing the results with those calculated from probabilistic analysis for the case of uniformly distributed ligands.[4] Then we examine, in a cell–substrate adhesion experiment, how the adhesion frequency (total and single-bond) and forward rate constant depend upon the number of ligands in a cluster, receptor aggregation on the microvilli, ligand density, receptor density, contact time, and binding pocket size.

MONTE CARLO MODEL DESCRIPTION

We use a microvillus-bearing cell (e.g., a human neutrophil or lymphocyte) as our model cell, i.e., we simulate a cell–substrate adhesion experiment in which a microvillus-bearing cell contacts a ligand-coated substrate with a known contact area for a known duration. The MC simulation described below is modified from a model developed by Mahama and Linderman.[16,17] We assume that only one type of receptor on the cell can react with the ligand on the substrate and the distance between the cell surface and substrate is constant. With little modification, this simulation can be applied to other types of cell adhesion experiments where receptors are distributed uniformly or more than one type of receptor interacts with the ligand.

When a microvillus-bearing cell contacts a ligand-coated substrate, it is very likely that the contact points are the tips of those microvilli that are abundant on the cell. In the case of human neutrophils, their microvilli contain most of L-selectin and P-selectin glycoprotein ligand-1 (PSGL-1) on their tips.[3,9,19] Adhesion will occur if bonds form during the contact between the cell and substrate. It is believed that two steps are involved in the formation of a receptor–ligand bond.[1,15] First, a receptor diffuses into the proximity of a ligand to form an encounter complex. This encounter complex then overcomes an energy barrier to form a bond, which is held together by a resultant of van der Waals forces, hydrogen bonding forces, electrostatic forces, and hydrophobic interactions. The apparent contact area between the cell and substrate is assumed to be $\sim 1\ \mu m^2$, so there are about five microvilli that are in touch with the substrate during each contact.[27] Thus one contact between the cell and substrate is simulated as five independent and simultaneous microvillus contacts with the substrate, where bonds form independently on individual microvilli.

For each individual microvillus, the contact area on the substrate is simulated as a flat circular region with radius R_{lg}. A plain square that has the same center as this circular contact region but has a larger area is selected as the simulation region on the microvillus. Figure 1 shows the two simulation regions that are put together as if a microvillus tip had contacted a

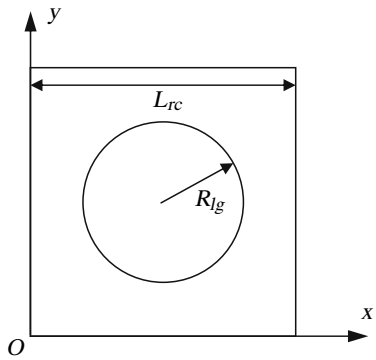

FIGURE 1. A schematic representation of the simulation region on the cell (square) and substrate (circle). L_{rc} is the side length of the square region and R_{lg} is the radius of the circular region. The circular region represents the contact area. The rectangular coordinate system is adopted in both regions.

substrate. The purpose of using a larger simulation region on the microvillus is to minimize the disturbance from the receptors around the edge of the contact region. If we assume that the simulation time or contact time is t^{contact}, and the characteristic time of diffusion is t_{d}, then the side length of the square can be calculated as,

$$L_{\text{rc}} = \max\left[2R_{\text{lg}} + d \cdot \left(t^{\text{contact}}/t_{\text{d}}\right),\ 500\,\text{nm}\right], \qquad (1)$$

where d is the binding pocket size. If the distance between a receptor and a ligand in the contact region is less than $d/2$, they will form an encounter complex. The characteristic time of diffusion t_{d} can then be calculated by[8]

$$t_{\text{d}} = \frac{d^2}{4D}, \qquad (2)$$

where D is the diffusion coefficient of the receptor.

The square simulation region is packed with circles of diameter d as shown in Fig. 2. This way of packing circles in a simulation region corresponds to a triangular grid with a lattice spacing of d. The indices inside each circle in Fig. 2 represent that circle's location and they are composed of an x index and a y index. The maximum y index is ny and the maximum x index is either nx (if its y index is odd) or $nx-1$ (if its y index is even). Note that different numbers of circles are present in adjacent rows. It is convenient to choose ny to be an even number (see explanation later in this section). The indices nx and ny are geometrically determined, respectively, by

$$nx = \text{an integer} \geq \frac{L_{\text{rc}}}{d}, \qquad (3)$$

and

$$ny = \text{an even integer} \geq \frac{2(L_{\text{rc}} - d)}{\sqrt{3}d} + 1. \qquad (4)$$

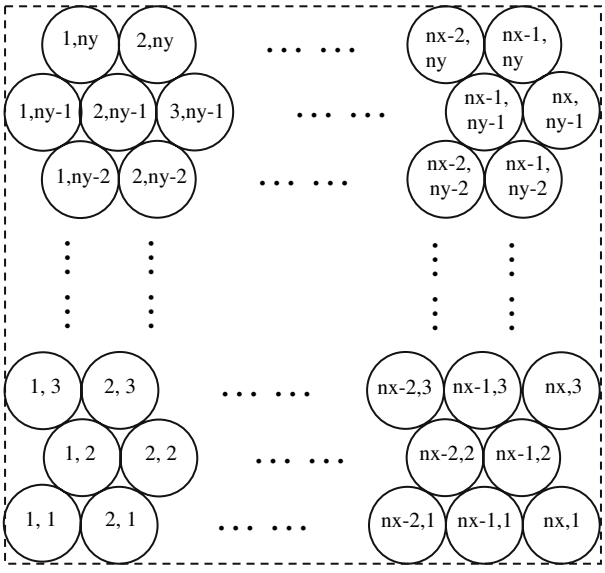

FIGURE 2. Triangular-grid packing of the square simulation region with circles of diameter *d* (binding pocket size). These circles represent possible locations of receptors and ligands. The numbers inside each circle are the indices of its location. The same packing scheme is used for both the cell and substrate.

On the substrate, the same number of circles is packed in the same manner as on the cell. In other words, a mirror image of the packed square simulation region is created. Note that, on the substrate, only the circles that have a distance less than R_{lg} from the center belong to the simulation region on the substrate.

In the simulation region on the cell, each circle in Fig. 2 represents a position that a receptor can possibly occupy. The Brownian motion of a receptor is modeled as its random motion from one circle to one of its six adjacent neighbors. Three events are involved in the simulation: diffusion of receptors, binding between receptors and ligands, and unbinding between receptors and ligands. These events are controlled by their characteristic times, the shortest of which is defined as the characteristic time of the simulation. The characteristic time of the simulation divided by the number of involved receptors yields the timestep of the simulation. During the simulation, a receptor is randomly chosen at every timestep. Whether it will move, bind to, or unbind from a ligand will be determined mainly by the characteristic time of that event as described below.

The simulation is initialized by placing some ligands or ligand clusters on the substrate (Fig. 3) and by placing some receptors on the cell surface. The location of each ligand or receptor is determined randomly by its two indices within the ranges defined by Eqs. 3 and 4. To accomplish this, we select a random integer (i) between 1 and $2nx-1$ and another random integer (j) between 1 and $ny/2$. Then the corresponding selected location in Fig. 2 is

$$(i,\ 2j) \text{ if } i \text{ is less than or equal to } nx - 1$$

or

$$(\mathrm{i} - nx\ +\ 1,\ 2j - 1) \text{ if } i \text{ is larger than } nx - 1.$$

This condition ensures that any location in Fig. 2 has an equal chance of being selected and is the reason why ny is chosen to be an even number. No ligand or

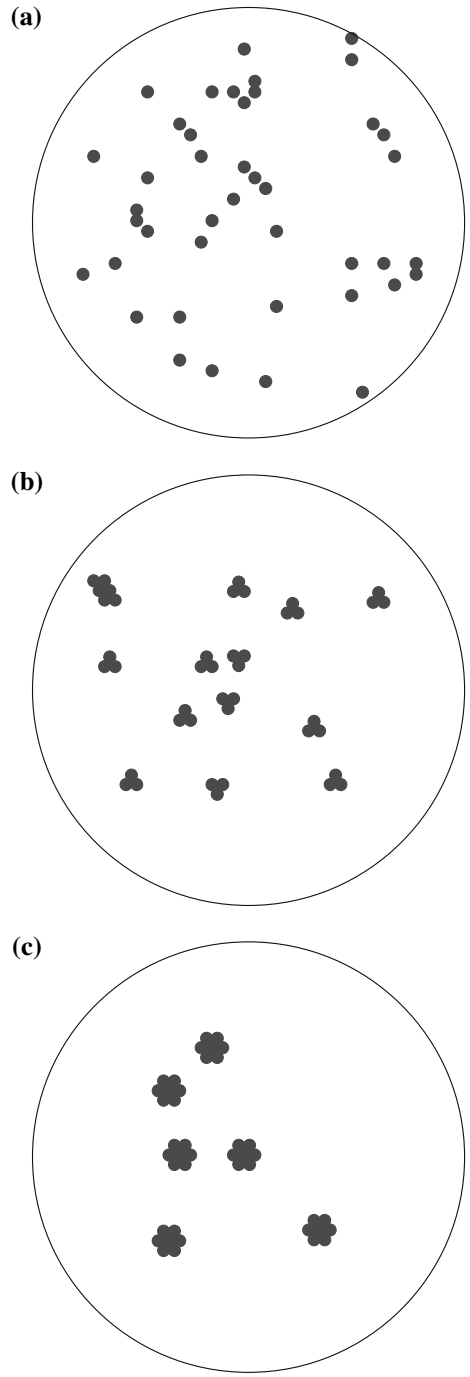

FIGURE 3. Representative ligand distribution in the contact area on the substrate: no clustering (a), three-ligand clustering (b), and seven-ligand clustering (c). The filled circles represent the distributed ligands. The average ligand densities in the whole contact area are approximately the same in all three cases.

receptor can occupy the same location in their corresponding simulation regions. After the receptor and ligand placement, the initial number of bonds is counted before any diffusion occurs by checking whether any receptor has the index of a ligand location in the contact area and whether a random number is less than the probability calculated by[12]

$$P_{\text{complex}\to\text{bond}} = 1 - e^{-k_+\Delta t}, \tag{5}$$

where k_+ is the on rate for an encounter complex to become a bond, $P_{\text{complex}\to\text{bond}}$ is the probability for an encounter complex to become a bond, and

$$\Delta t = \min\left(t^{\text{complex}},\ t^{\text{contact}} - t_0\right), \tag{6}$$

where t_0 is the time instant when the complex is formed and t^{complex} is the average time for a complex to endure as a complex. In this simulation, t^{complex} is assumed to be equal to $(d/2)^2/4D$.

After this initial check, a receptor is chosen randomly at every Monte Carlo timestep. Whether this chosen receptor moves at this timestep is determined by a probability calculated as the ratio of the characteristic time of simulation and diffusion. If the receptor does not move, the simulation goes on to the next timestep. If it does move, a random adjacent location is selected for it to move into. If the new location is already occupied by either a free receptor or a bound receptor, then the move is rejected (this does not happen often in our simulation where moderate receptor and ligand densities are used). If the new location is beyond the boundary, a periodic condition is imposed and this receptor appears on the other side of the simulation region. If the new location is empty, the current location is unoccupied and the receptor moves to the new location. If this new location is a free ligand location that is inside the contact area, an encounter complex forms, and whether this encounter complex can evolve into a bond is determined by the probability calculated with Eq. 5. After every bond formation, a new receptor is added at the boundary of the square simulation region as soon as an amount of time t_d passes.

After a bond forms, the probability for this bond to dissociate into an encounter complex at every timestep can be calculated with

$$P_{\text{break}} = 1 - e^{-k_-\Delta s}, \tag{7}$$

where k_- is the off rate of the bond and Δs is the timestep of the simulation. Once a bond dissociates into an encounter complex, the probability of re-binding is calculated with Eq. 5. If no re-binding occurs, this pair of receptor and ligand is re-categorized as unbound or free.

For each cell–substrate contact, the same simulation procedure is run for each microvillus individually. The bonds that remain at the end of the contact for each

microvillus are added up to a total number of bonds, which will allow us to determine whether there is an adhesion event and whether it is a single-bond or multiple-bond event. For each set of parameters, we usually simulate 50 cell–bead pairs. For each cell–substrate pair, one hundred contacts, if not specified otherwise, are simulated. The total and single-bond adhesion frequencies are calculated by dividing the total number of adhesion events and the total number of single-bond events, respectively, by the total number of contacts. The single-bond percentage for each cell–substrate pair is calculated by dividing the total number of sing-bond events by the total number of adhesion events.

In the simulation, different combinations of ligand density (C_L), receptor density (C_R), contact time ($t^{contact}$), and binding pocket size (d) were used while other parameters were kept as constants: $D = 1000\ nm^2/s$, $k_+ = 200\ s^{-1}$, $k_- = 1\ s^{-1}$, and $R_{lg} = 50$ nm. The default values for C_L, C_R, $t^{contact}$, and d were $C_L = 200\ \mu m^{-2}$, $C_R = 200\ \mu m^{-2}$, $t^{contact} = 0.1$ s, and $d = 5$ nm. The simulation program was written in *C* (CodeWarrior, Metrowerks, Austin, TX) and it took about 30 s on a Windows PC (Pentium IV, 3.2 GHz) to run one simulation with the default parameters (100 contacts for 50 cell–substrate pairs). However, if contact time was increased to 4 s while other parameters were unchanged, it took five and a half days to run 100 contacts for 50 cell–substrate pairs.

PROBABILISTIC KINETIC MODEL

In the case of uniformly distributed ligands and receptors, there exists a probabilistic exact solution for calculating the adhesion frequency of such cell–substrate or cell–cell adhesion experiments.[4] This probabilistic solution will allow us to compare our MC simulation results with those calculated from probabilistic analysis, which will be described in this section. Overall, if the forward and reverse rate constants are k_f and k_r, respectively, the association equilibrium constant (K_a) can be calculated by

$$K_a = \frac{k_f}{k_r}. \tag{8}$$

The probability of forming n ($n = 0, 1, 2, ...$) receptor–ligand bonds on one microvillus tip after contact time t, $p_n(t)$, is of the form of the Poisson distribution[4]

$$p_n(t) = \frac{\langle n\rangle^n}{n!}\exp(-\langle n\rangle), \tag{9}$$

where $\langle n\rangle$ is the average number of bonds, given by

$$\langle n\rangle = A_c C_R C_L K_a[1 - \exp(-k_r t)] \tag{10}$$

and A_c is the contact area between the microvillus and substrate.

The question of interest now is how to calculate the total and single-bond adhesion frequenies for the contact made by five microvilli given the probability for each microvillus contact. If there are N_m microvilli in contact with the substrate during each cell–substrate contact and every microvillus contacts the substrate independently, the total adhesion frequency is given by

$$p_a(t) = 1 - (p_0(t))^{N_m} = 1 - \exp(-N_m\langle n\rangle), \tag{11}$$

and the single-bond adhesion frequency is given by

$$p_1(t) = N_m p_1(t)(p_0(t))^{N_m - 1} = N_m\langle n\rangle \exp(-N_m\langle n\rangle). \tag{12}$$

Note that

$$\begin{aligned} N_m\langle n\rangle &= N_m A_c C_R C_L K_a\left[1 - \exp\left(-k_r t\right)\right] \\ &= A_{total} C_R C_L K_a\left[1 - \exp\left(-k_r t\right)\right] \end{aligned}, \tag{13}$$

where $A_{total} = N_m A_c$ is the total contact area between the substrate and N_m microvilli on the cell. Therefore, the total and single-bond adhesion frequency can be directly calculated as if the cell contacts the substrate by one area that is equal to the total surface area of all the microvillus tips.

RESULTS

Dependence of Adhesion Frequency on Ligand and Receptor Density

In our simulation, if ligands were randomly distributed on the substrate without clustering as shown in Fig. 3a, the total adhesion frequency increased when ligand or receptor density was increased (Fig. 4a). However, the corresponding single-bond adhesion frequency first increased and then decreased after reaching the maximum. In fact, the single-bond percentage decreased monotonically as shown in Fig. 4b, indicating the presence of more and more multiple-bond adhesion events as ligand or receptor density was increased. If receptor density was increased from 100 to 3000 μm^{-2} while ligand density was kept at 200, 800, or 3000 μm^{-2}, almost identical results as shown in Fig. 4a were obtained (data not shown), which was expected according to first order kinetics.

For randomly distributed ligands on the substrate, the total and single-bond adhesion frequency could also be calculated with Eqs. 11 and 12. This calculation would allow us to compare our MC simulation with probabilistic analysis and it requires k_f and k_r to be

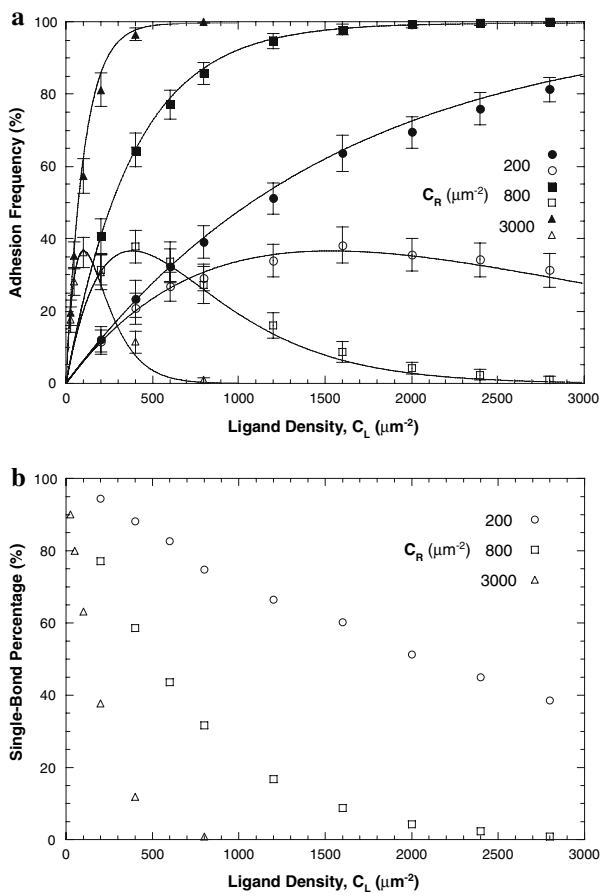

FIGURE 4. Dependence of the total and single-bond adhesion frequencies (a) and the single-bond percentage (b) on ligand density at three different receptor densities (circle: C_R = 200 μm^{-2}; square: C_R = 800 μm^{-2}; triangle: C_R = 3000 μm^{-2}). In (a), the solid lines are the predictions computed from probabilistic analysis and the filled and open symbols represent the total and single-bond adhesion frequency, respectively. Here, all ligands are uniformly distributed on the substrate. All the error bars shown in this figure and the following figures represent the standard deviations.

known *a priori*. To estimate k_f, we recorded the average rate of bond formation in a very short period of time (0.1 s) while setting the bond lifetime at 100 s (other parameters were at default). We found an average bond formation rate of 1.346 bonds per contact per second. Since the average diameter of the microvillus tip was assumed to be about 100 nm, k_f could be estimated with first order kinetics to be about 857 nm^2/s. To estimate k_r, we placed 200 bonds in the total contact area with no free receptors or ligands and recorded the average bond dissociation rate in a very short period of time (0.01 s; other parameters were at default). On average, there were 1.48 bonds broken, from which k_r was estimated to be about 0.739 s^{-1}, which yielded a K_a of about 1160 nm^2. As shown in Fig. 4a, our MC simulation agrees very well with probabilistic analysis. If the total adhesion frequency was less than 20%, most of the adhesion events were mediated by only one bond. This finding is consistent with previous ones.[4,21] However, it should be noted that low adhesion frequency did not guarantee single bonds (data not shown). Even at a total adhesion frequency of 5%, multiple-bond adhesion events still occurred, as shown in an earlier simulation.[26]

Effect of Microvilli

When a microvillus-bearing cell touches a ligand-coated substrate, the contact points will very likely be the microvillus tips, which are usually abundant on the cell surface. In the case of human neutrophils, most of L-selectin and PSGL-1 are located on the microvillus tips to facilitate their adhesion to other surfaces.[3,9] Therefore, one obvious advantage of receptor aggregation on the microvillus tip is to present these receptors to their ligands on the opposing surface so that they can be recognized easily. It has been hypothesized that receptor aggregation may increase local receptor density, thus leading to higher adhesion frequency. To investigate this hypothesis, we conducted our MC simulation by distributing the total number of receptors in the whole apparent contact area (1 μm^2), i.e., removing the microvilli to smoothen the cell surface and re-distributing the receptors randomly in the whole apparent contact area. As shown in Fig. 5a, the total and single-bond adhesion frequencies depend on receptor and ligand density in a very similar fashion as in Fig. 4a where receptors were distributed on five microvilli. This indicates that it is the number of receptors in the contact area, whether receptor density and contact area are large or small, that determines the total and single-bond adhesion frequencies as shown in Eqs. 10 and 13. However, it should be noted that, although our results in Fig. 5a agree well with the ones calculated from Eqs. 11 and 12, this conclusion is true only when the receptors on the microvilli are not so crowded to become clusters as shown in Fig. 3.

Although receptor aggregation on the microvillus tip did not affect the total adhesion frequency much, it did have a profound effect on the forward rate constant when receptor density was increased and ligand density was kept at 200 μm^{-2}, as shown in Fig. 5b. When ligand density was kept at 800 or 3000 μm^{-2}, the results had similar trends as shown in Fig. 5b (data not shown). In the absence of microvilli, i.e., when the receptors on the microvilli were randomly distributed in the whole contact area, the forward rate constant increased as receptor density was increased. This was expected since, on average, more receptors were surrounding one ligand as receptor density was increased.[15] However, in the presence of

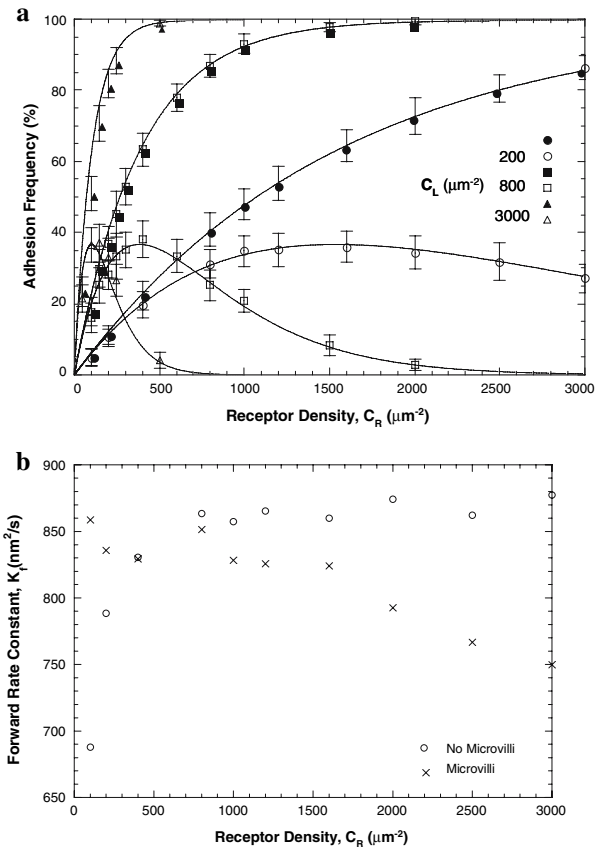

FIGURE 5. Dependence of the total and single-bond adhesion frequency (a) and the forward rate constant (b) on receptor density at several different ligand densities (circle: C_L = 200 μm^{-2}; square: C_L = 800 μm^{-2}; triangle: C_L = 3000 μm^{-2}) when receptors were randomly distributed in the whole 1-μm^2 contact area (i.e., both cell and substrate surfaces were flat and receptors were randomly distributed in the whole contact area). The filled and open symbols represent data from MC simulation while the solid lines represent the corresponding results from probabilistic analysis. All ligands were randomly distributed without clustering on the substrate.

microvilli, the forward rate constant decreased as receptor density was increased. This is likely due to the fact that there were only a few ligands on the substrate available to each microvillus tip. Once a bond was formed, it would very likely stay bound during the short contact time (0.1 s) because of its long lifetime (about 1.35 s). In the absence of microvilli, this would only cause a very small change in ligand density (0.5%). However, in the presence of microvilli, this would cause a much larger change in ligand density (~12.7%). Consequently, this would cause a more significant drop in the overall bond formation rate and the forward rate constant. In the extreme case of only one ligand available to one microvillus tip, once a bond was formed, even though other receptors could diffuse into the vicinity of this ligand, no bonds could form until this bond was broken. In essence, two trends were competing with each other to influence the overall forward rate constant during this binding process: the increase in the forward rate constant due to the increase in receptor density and the decrease in the forward rate constant due to the decrease in the number of ligands available for binding. In the absence of microvilli, the former was dominant; in the presence of microvilli, the latter was dominant.

Two more facts are worthy of notice in Fig. 5b. The difference in the forward rate constant with or without microvilli at different receptor densities is likely the reason for the slight difference between the simulation results in Figs. 4a and 5a. When receptor density is small, receptor aggregation on the microvillus does increase the forward rate constant.

Effect of Ligand Clustering

If receptor density was kept at 200 μm^{-2} and ligands were randomly distributed on the substrate in clusters of three or seven as shown in Fig. 3b and c, the total adhesion frequency increased when ligand density was increased (Fig. 6a). When receptor density or contact time was increased, the total adhesion frequency also increased in the presence of ligand clustering (data not shown). In both cases of clustered ligands, clustering decreased both the total and single-bond adhesion frequency, but increased the percentage of single-bond adhesion events at the same ligand density (Fig. 6b). It is clear that, even in the presence of clustering, most of the adhesion events were still mediated by a single bond if the total adhesion frequency was less than 20%.

Ligand clustering also affected the forward rate constant significantly. At the receptor density of 200 μm^{-2}, the forward rate constant decreased as clustering increased as shown in Fig. 6c. However, the decrease in the forward rate constant caused by the increase in ligand density became less noticeable as clustering increased. This is probably because whenever clustered ligands were available to a microvillus, they would be present in groups of three or seven. As a result, formation of just one bond should not hinder the formation of more new bonds as in the case of no clusters. The simulation described in this section was also conducted at the receptor density of 400 μm^{-2}, the same conclusions could be drawn about ligand clustering (data not shown).

Dependence of Adhesion Frequency on Contact Time

When contact time was increased, receptors could travel further, and thus have better chances to encounter ligands and form more bonds. As a result, higher adhesion frequency was expected. As shown in

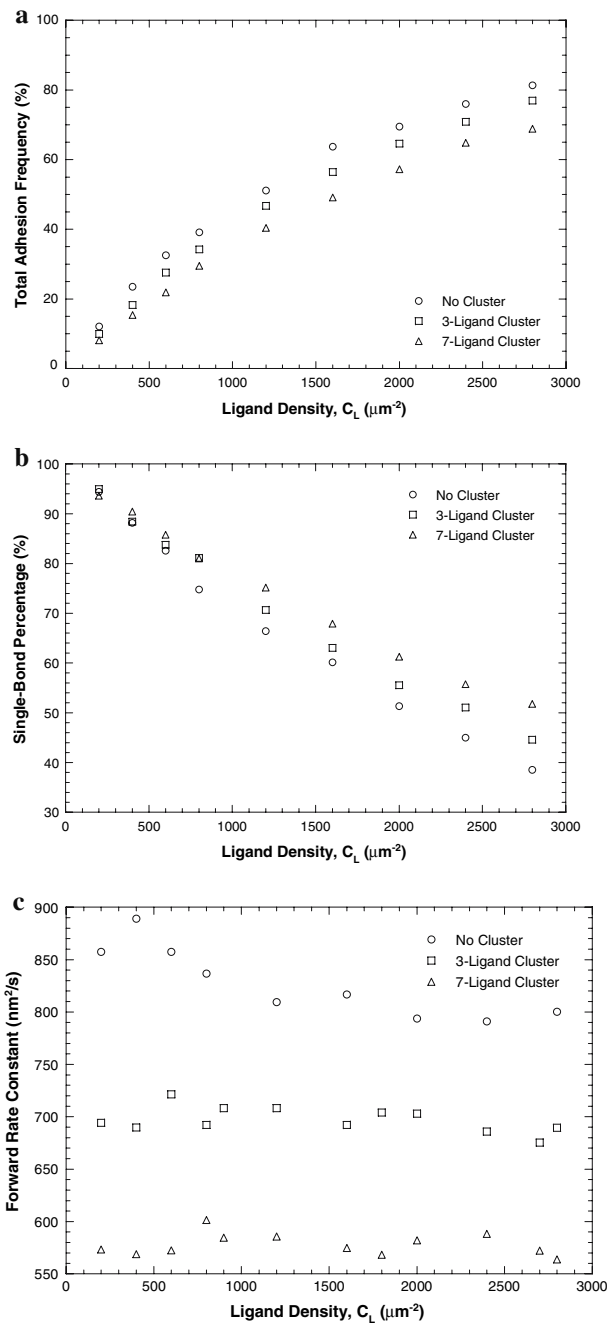

FIGURE 6. Dependence of the total and single-bond adhesion frequencies (a), the single-bond percentage (b), and the forward rate constant (c) on ligand density and cluster size (clusters of 1, 3, and 7) at the receptor density of 200 μm^{-2}.

Fig. 7, the total and single-bond adhesion frequencies increased quickly when contact time was increased. When more receptors and/or ligands were present in the contact area, it took shorter periods of time to reach stable adhesion frequencies. Eventually, the single-bond adhesion frequency reached the maximum and then decreased. The adhesion was dominated by single-bond events if the adhesion frequency was less than 20% and the percentage of single-bond adhesion events decreased monotonically as contact time was increased.

At the contact times longer than 0.5 s, our MC simulation does not agree well with probabilistic analysis. The total adhesion frequency is smaller than the one predicted from probabilistic analysis and the single-bond adhesion frequency is larger. This discrepancy is likely due to the decrease in the forward rate constant when contact time was increased. Even with five microvilli in the contact area, the total contact area was only about 0.039 μm^2 and the total number of receptors that can bind to ligands was only about seven. When contact time became longer, more bonds would form and the decrease in ligand density would become more prominent. As a result, the forward rate constant would be much smaller. For example, at the ligand density of 800 μm^{-2} (Fig. 7), the average bond formation rate at the contact time of 2 s decreased significantly to about 502 nm^2/s compared with 857 nm^2/s at the contact time of 0.1 s. If this rate of 502 nm^2/s was used in the probabilistic analysis, the total and single-bond adhesion frequency would be 96 and 12%, respectively, which are in very good agreement with our MC simulation. Note that the actual instantaneous forward rate constant at 2 s should be even smaller since 502 nm^2/s was estimated from the average bond formation rate in the whole 2-s contact time.

After clustered ligands of 3 or 7 were distributed in the contact area, both the total and single-bond adhesion frequencies decreased as contact time and clustering increased. In both cases of clustering, adhesion was dominated by single-bond adhesion events if the total adhesion frequencies was less than 20% and the single-bond percentage decreased monotonically as contact time was increased. However, the percentage of single-bond adhesion events at the same contact time with ligand clustering was consistently larger than without ligand clustering (data not shown).

Dependence of Adhesion Frequency on Binding Pocket Size

The binding pocket size (d) is an important factor because it represents how close receptors and ligands need to become in the contact region before they can form an encounter complex. As expected, the total and single-bond adhesion frequencies decreased and increased, respectively, when a smaller and larger binding pocket size was employed in the simulation (Fig. 8). Because of the smaller or larger binding pocket, there was less or more opportunity for receptors to form encounter complexes with ligands, hence resulting in lower or higher adhesion frequency. After

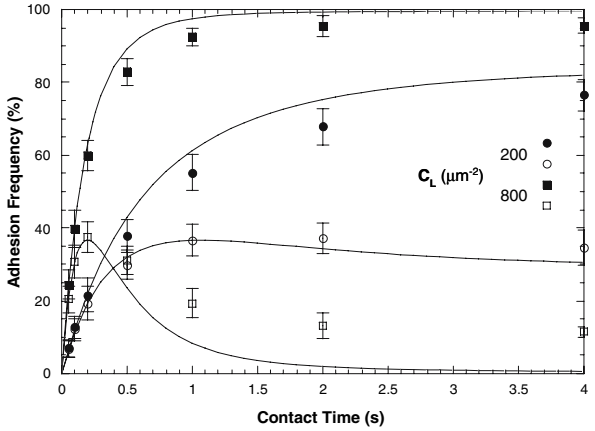

FIGURE 7. Dependence of the total and single-bond adhesion frequencies on contact time at different ligand densities (the receptor density $C_R = 200\ \mu m^{-2}$). The filled and open symbols represent the total and single-bond adhesion frequencies from MC simulation, respectively. The solid lines represent the corresponding results from probabilistic analysis. Here, all ligands were uniformly distributed on the substrate. For the cases where $t^{contact} \geq 2$ s, we only simulated 5 cell–substrate pairs and 100 contacts for each pair to reduce computational time.

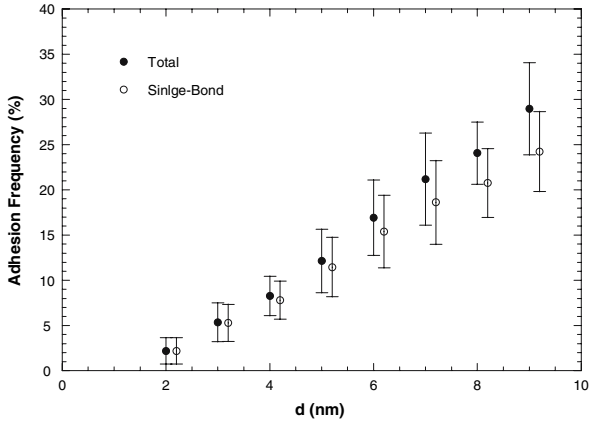

FIGURE 8. Dependence of the total and single-bond adhesion frequencies on binding pocket size (*d*). For clarity, the single-bond adhesion frequency is plotted intentionally at the binding pocket sizes that are 0.2-nm larger than their actual values.

ligand clustering was introduced in the simulation, this opportunity was diminished (data not shown), so there were fewer adhesion events. In general, the single-bond percentage was always larger in the presence of ligand clustering. For all the parameters considered in this case, all adhesion events were dominated by single bonds because their total adhesion frequencies were less than or just a little larger than 20%.

DISCUSSION

We successfully carried out a Monte Carlo simulation of the adhesion between a microvillus-bearing cell and a ligand-coated substrate. In the cases where receptors and ligands were uniformly distributed and the forward and reverse rate constants did not change much, our MC simulation agreed very well with probabilistic analysis, thus validating our modeling approach. Our simulation showed that, in the presence of ligand clustering on the substrate, low adhesion frequency ($< 20\%$) could still be used as an indicator for single bonds in a cell–substrate or cell–bead adhesion experiment. This criterion held true even when we varied the parameters like the number of ligands in a cluster, ligand density, receptor density, contact time, and binding pocket size. Even at very large total adhesion frequencies, single bonds were still present (Figs. 4–7). However, even a frequency as low as 5% could not guarantee single bonds in a cell–substrate adhesion event; this reflects the stochastic nature of the receptor–ligand binding mechanism. Multiple bonds in any experimental measurement will increase the force necessary to rupture the adhesion or increase the lifetime of the adhesion subjected to a constant separating force, so these bonds should show up as outliers.

In our simulation, we ignored the details of the microvillus geometry and did not include the dependence of the forward rate constant on the separation distance.[6,12] Electron micrographs have shown that microvillus tips usually have curved surfaces with curvature radii close to the lengths of proteins,[2,3,19] i.e., on the order of tens of nanometers. Therefore, once a microvillus contacts a substrate, most of the adhesion molecules (if not all) are able to interact with the molecules on the substrate. Many factors may influence how fast the interaction can occur, including separation distance, molecular stiffness, and membrane or surface compliance. From this perspective, every individual molecule has a slightly different forward rate constant. In our simulation, the forward rate constant of each molecule is like the average forward rate constant of all the molecules involved. If these factors were included in our simulation, our results would probably show more variability, but our major conclusions would very likely remain the same.

Our simulation also showed that ligand clustering decreased the total adhesion frequency but increased the single-bond adhesion frequency if other parameters were kept constant. These effects are very likely due to the decreased forward rate constant as shown in Fig. 6c. In most of our simulations, since ligand density was not very large, only a limited number of ligands were available on the substrate and they could form clusters of three or seven. For all the parameters considered in the simulation (Figs. 4–8), the multiple-bond adhesion frequency always increased as the total adhesion frequency increased. However, the single-

bond adhesion frequency reached its maximum value when the total adhesion frequency was around 50%, then decreased. Therefore, if a substrate is prepared with small clusters of ligands on it, these clusters will promote more single-bond adhesion events during an adhesion experiment. When one studies the effect of clustering, it is of great importance to take into account different factors that affect the adhesion frequency including cluster size.

A similar clustering mechanism can be found in the case of neutrophil rolling on the endothelium where L-selectin and PSGL-1 are concentrated on the microvillus tips. Although these molecules are not in clusters of 3 or 7 like the ligands in our simulation, they still represent a concentrated distribution on the whole cellular surface. At small receptor and ligand densities (C_R = 100 μm^{-2} and C_L = 200 μm^{-2}), this concentrated distribution might help the neutrophil to adhere to the endothelium with an increased forward rate constant (Fig. 5b), but the difference in the total adhesion frequency was found to be very small (5.1 versus 6.3%) (Fig. 5a). At other receptor and ligand densities considered, the forward rate constants did not differ much from each other. Hence we conclude that the prediction from probabilistic analysis, viz., that the number of receptors in the contact area determines the total and single-bond adhesion frequency (Eqs. 10–13), holds very well. In other words, the microvilli do not add additional adhesion efficiency from a kinetics perspective (Figs. 4a and 5a). Nevertheless, their existence on cell surfaces can be justified with many other functions. For example, they provide excess membrane area when leukocytes pass small capillaries so that leukocytes can deform easily;[10,29] they are theoretically predicted to penetrate the endothelial glycocalyx so that the molecules on their tips can gain access to the molecules on the endothelium;[30] in addition, they supply a natural ready-to-use lever arm to stabilize leukocyte rolling in the absence of tether extraction.[20]

At C_R = 200 μm^{-2} and C_L = 200 μm^{-2}, the forward rate constant can be estimated with the theoretical approach developed by Bell,[1] but a value three times that of our MC simulation was obtained. If we replace the rate constant for encounter-complex formation in the Bell approach by $2\pi D/\ln(2b/d)$ (b is one-half the mean distance between ligands), as developed by Lauffenburger and Linderman,[15] a reasonable estimate would be obtained ($\sim$872 nm^2/s). Nevertheless, current theoretical formulation does not explain the dependence of the forward rate constant on receptor density. For two flat contact surfaces without microvillus-like structures, the forward rate constant increased as receptor density was increased (Fig. 5b). This is anticipated since larger receptor density will make it easier to form bonds. However, the presence of microvilli in our simulation affected the forward rate constant in a counterintuitive fashion, i.e., the forward rate constant decreased as receptor density was increased (Fig. 5b). This is probably due to the fact that the microvillus tip is so small that the continuum approach no longer applies. Therefore, a more appropriate theoretical framework is necessary for the kinetic treatment of the adhesion between a microvillus-bearing cell and a ligand-coated substrate.

With little modification, this simulation can be applied to other cell–substrate or cell–bead adhesion experiments or to the cases where multiple pairs of receptors and ligands are present. Combined with experimental data, this type of simulation may help us extract some valuable information such as the on and off rates of receptor–ligand interactions. This is very similar to the methodology proposed and adopted by Chesla et al.[4] They employed probabilistic analysis to determine the two-dimensional receptor–ligand binding kinetics (the overall rate constants) by carefully measuring the adhesion probability or frequency. In future simulations, receptor clustering on the cell could be included. The dependence of the off rate on the magnitude or the loading rate of a mechanical force, as well as multivalency and cell surface heterogeneity, could also be included. As shown in our simulation, the forward rate constant may not be an intrinsic constant parameter that is appropriate for describing receptor–ligand interactions. Thus the real power of our MC simulation may lie in its ability to examine various theoretical analyses of kinetic processes and identify true intrinsic parameters that govern these processes.

ACKNOWLEDGMENTS

This work was supported by the National Institutes of Health (R01 HL069947 and R21/R33 RR017014), the Whitaker Foundation (RG-99-0289), and the National Natural Science Foundation of China. We thank Dr. Salvatore P. Sutera for his critical reading of the manuscript.

REFERENCES

[1] Bell, G. I. Models for the specific adhesion of cells to cells *Science* 200:618–627, 1978.

[2] Bruehl, R. E., K. L. Moore, D. E. Lorant, N. Borregaard, G. A. Zimmerman, R. P. McEver, and D. F. Bainton. Leukocyte activation induces surface redistribution of P-selectin glycoprotein ligand-1. *J. Leukoc. Biol.* 61:489–499, 1997.

[3] Bruehl, R. E., T. A. Springer, and D. F. Bainton. Quantitation of L-selectin distribution on human leukocyte microvilli by immunogold labeling and electron microscopy. *J. Histochem. Cytochem.* 44:835–844, 1996.

[4]Chesla, S. E., P. Selvaraj, and C. Zhu. Measuring two-dimensional receptor–ligand binding kinetics by micropipette. *Biophys. J.* 75:1553–1572, 1998.
[5]Cozens-Roberts, C., J. A. Quinn, and D. A. Lauffenburger. Receptor-mediated cell attachment and detachment kinetics: I. Probabilistic model and analysis. *Biophys. J.* 58:841–856, 1990.
[6]Dembo, M., D. C. Torney, K. Saxman, and D. Hammer. The reaction-limited kinetics of membrane-to-surface adhesion and detachment. *Proc. R. Soc. Lond.* B234:55–83, 1988.
[7]Dustin, M. L., L. M. Ferguson, P.-Y. Chan, T. A. Springer, and D. E. Golan. Visualization of CD2 interaction with LFA-3 and determination of the two-dimensional dissociation constant for adhesion receptors in a contact area. *J. Cell Biol.* 132:465–474, 1996.
[8]Einstein, A. Investigations on the Theory of the Brownian Movement (edited with notes by R. Fürth and translated by A. D. Cowper). Dover Publications Inc, New York.
[9]Erlandsen, S. L., S. R. Hasslen, and R. D. Nelson. Detection and spatial distribution of the β_2 integrin (Mac-1) and L-selectin (LECAM-1) adherence receptors on human neutrophils by high-resolution field emission SEM. *J. Histochem. Cytochem.* 41:327–333, 1993.
[10]Evans, E. and A. Yeung. Apparent viscosity and cortical tension of blood granulocytes determined by micropipette aspiration. *Biophys. J.* 56:151–160, 1989.
[11]Gutfreund, H. Kinetics for the Life Sciences: Receptors, Transmitters and Catalysts. Cambridge University Press, New York.
[12]Hammer, D. A., and S. M. Apte. Simulation of cell rolling and adhesion on surfaces in shear flow: General results and analysis of selectin-mediated neutrophil adhesion. *Biophys. J.* 63:35–57, 1992.
[13]Irvine, D. J., K. A. Hue, A. M. Mayes, and L. G. Griffith. Simulations of cell-surface integrin binding to nanoscale-clustered adhesion ligands. *Biophys. J.* 82:120–132, 2002.
[14]Kruk, P. J., H. Korn, and D. S. Faber. The effects of geometrical parameters on synaptic transmission: A Monte Carlo simulation study. *Biophys. J.* 73:2874–2890, 1997.
[15]Lauffenburger, D. A. and J. J. Linderman. Receptors: Models for BindingTrafficking, and Signaling. Oxford University Press, New York.
[16]Mahama, P. A., and J. J. Linderman. A Monte Carlo study of the dynamics of G-protein activation. *Biophys. J.* 67:1345–1357, 1994.
[17]Mahama, P. A. and J. J. Linderman. Monte Carlo simulations of membrane signal transduction events: Effect of receptor blockers on G-protein activation. *Ann. Biomed. Eng.* 23:299–307, 1995.
[18]McQuarrie, A. D. Kinetics of small systems I *J. Chem. Phys.* 38:433–436, 1963.
[19]Moore, K. L., K. D. Patel, R. E. Bruehl, F. Li, D. A. Johnson, H. S. Lichenstein, R. D. Cummings, D. F. Bainton, and McEver. P-selectin glycoprotein ligand-1 mediates rolling of human neutrophils on P-selectin. *J. Cell Biol.* 128:661–671, 1995.
[20]Park, E. Y., M. J. Smith, E. S. Stropp, K. R. Snapp, J. A. DiVietro, W. F. Walker, D. W. Schmidtke, S. L. Diamond, and M. B. Lawrence. Comparison of PSGL-1 microbead and neutrophil rolling: Microvillus elongation stabilizes P-selectin bond clusters. *Biophys. J.* 82:1835–1847, 2002.
[21]Piper, J. W., R. A. Swerlick, and C. Zhu. Determining force dependence of two-dimensional receptor–ligand binding affinity by centrifugation. *Biophys. J.* 74:492–513, 1998.
[22]Riley, M. R., H. M. Buettner, F. J. Muzzio, and S. C. Reyes. Monte Carlo simulation of diffusion and reaction in two-dimensional cell structures. *Biophys. J.* 68:1716–1726, 1995.
[23]Saxton, M. J. Anomalous diffusion due to obstacles: A Monte Carlo study *Biophys. J.* 66:394–401, 1994.
[24]Saxton, M. J. Anomalous diffusion due to binding: A Monte Carlo study. *Biophys. J.* 70:1250–1262, 1996.
[25]Shao, J. Y. Measuring Piconewton Forces with Micropipette Suction and its Application to the Flow and Adhesion of Individual Neutrophils. Duke University, Durham, North Carolina, 1997.
[26]Shao, J. Y., and R. M. Hochmuth. Mechanical anchoring strength of L-selectin, β_2 integrins and CD45 to neutrophil cytoskeleton and membrane. *Biophys. J.* 77:587–596, 1999.
[27]Shao, J. Y., H. P. Ting-Beall, and R. M. Hochmuth. Static and dynamic lengths of neutrophil microvilli. *Proc. Natl. Acad. Sci. USA* 95:6797–6802, 1998.
[28]Shao, J. Y., G. Xu, and P. Guo. Quantifying cell-adhesion strength with micropipette manipulation: Principle and application. *Front. Biosci.* 9:2183–2191, 2004.
[29]Ting-Beall, H. P., D. Needham, and R. M. Hochmuth. Volume and osmotic properties of human neutrophils. *Blood* 81:2774–2780, 1993.
[30]Zhao, Y., S. Chien, and S. Weinbaum. Dynamic contact forces on leukocyte microvilli and their penetration of the endothelial glycocalyx. *Biophys. J.* 80:1124–1140, 2001.
[31]Zhu, C., M. Long, S. E. Chesla, and P. Bongrand. Measuring receptor/ligand interaction at the single-bond level: Experimental and interpretative issues. *Ann. Biomed. Eng.* 30:305–314, 2002.